Video Article

Micropipette Aspiration of Substrate-attached Cells to Estimate Cell Stiffness

Myung-Jin Oh[1], Frank Kuhr[1], Fitzroy Byfield[2], Irena Levitan[1]

[1]Section of Respiratory, Critical Care and Sleep Medicine, Department of Medicine, University of Illinois

[2]Institute for Medicine and Engineering, University of Pennsylvania

Correspondence to: Irena Levitan at levitan@uic.edu

URL: https://www.jove.com/video/3886
DOI: doi:10.3791/3886

Keywords: Bioengineering, Issue 67, Biophysics, Biomedical Engineering, Medicine, Cellular Biology, Cell stiffness, biomechanics, microaspiration, cell membrane, cytoskeleton

Date Published: 9/27/2012

Citation: Oh, M.J., Kuhr, F., Byfield, F., Levitan, I. Micropipette Aspiration of Substrate-attached Cells to Estimate Cell Stiffness. *J. Vis. Exp.* (67), e3886, doi:10.3791/3886 (2012).

Abstract

Growing number of studies show that biomechanical properties of individual cells play major roles in multiple cellular functions, including cell proliferation, differentiation, migration and cell-cell interactions. The two key parameters of cellular biomechanics are cellular deformability or stiffness and the ability of the cells to contract and generate force. Here we describe a quick and simple method to estimate cell stiffness by measuring the degree of membrane deformation in response to negative pressure applied by a glass micropipette to the cell surface, a technique that is called Micropipette Aspiration or Microaspiration.

Microaspiration is performed by pulling a glass capillary to create a micropipette with a very small tip (2-50 μm diameter depending on the size of a cell or a tissue sample), which is then connected to a pneumatic pressure transducer and brought to a close vicinity of a cell under a microscope. When the tip of the pipette touches a cell, a step of negative pressure is applied to the pipette by the pneumatic pressure transducer generating well-defined pressure on the cell membrane. In response to pressure, the membrane is aspirated into the pipette and progressive membrane deformation or "membrane projection" into the pipette is measured as a function of time. The basic principle of this experimental approach is that the degree of membrane deformation in response to a defined mechanical force is a function of membrane stiffness. The stiffer the membrane is, the slower the rate of membrane deformation and the shorter the steady-state aspiration length.The technique can be performed on isolated cells, both in suspension and substrate-attached, large organelles, and liposomes.

Analysis is performed by comparing maximal membrane deformations achieved under a given pressure for different cell populations or experimental conditions. A "stiffness coefficient" is estimated by plotting the aspirated length of membrane deformation as a function of the applied pressure. Furthermore, the data can be further analyzed to estimate the Young's modulus of the cells (E), the most common parameter to characterize stiffness of materials. It is important to note that plasma membranes of eukaryotic cells can be viewed as a bi-component system where membrane lipid bilayer is underlied by the sub-membrane cytoskeleton and that it is the cytoskeleton that constitutes the mechanical scaffold of the membrane and dominates the deformability of the cellular envelope. This approach, therefore, allows probing the biomechanical properties of the sub-membrane cytoskeleton.

Video Link

The video component of this article can be found at https://www.jove.com/video/3886/

Protocol

1. Pulling Glass Micropipettes

Equipment: Micropipette Puller, Microforge.

Glass: Boroscillicate glass capillaries (~1.5 mm external diameter, ~1.4 mm internal diameter).

1. **Micropipettes are pulled** using the same basic approach that is used to prepare glass microelectrodes for electrophysiology recordings. Briefly, a glass capillary is heated in the middle and when the glass starts to melt the two halves of the capillary are pulled apart generating two micropipettes. Multiple commercial pullers are available to perform this process ranging from relatively simple vertical pullers that use gravity to pull the two pipettes apart to highly-sophisticated horizontal pullers that offer multiple programmable options to vary the velocity and other parameters of the pull. Both types of pullers were used in our experiments.
2. **Requirements for the geometry of the pipette tip**: The tips of the pipettes used in these experiments typically range between 2 to 6 μm external diameter depending on the size of the cell. Another important parameter is the shape of the tip, which should approximate a cylindrical tube (see **Figure 1**). This can be achieved by optimizing the parameters of the pull and verifying the shape of the tip under the microscope until the desired shape is obtained. The optimal length of the pipette shank depends on the amount of expected deformation: if the deformations are small <10 μm, it is enough that the cylinder-like part of the pipette is also relative short (the same order of magnitude),

for larger deformations adjust accordingly. In general, increasing the heat and/or increase in "pull" decreases the diameter of the tip. The increase in "pull" also generates a tip with a longer taper. In our experiments, using a Sutter P-97 horizontal pipette puller, the program was optimized to the following parameters: Heat of 473; Pull 22; Velocity 22, Time 200; Pressure 500. It is also possible to create cylindrical tips by pulling a very long shank and then breaking and polishing it. Detailed instructions of how to prepare different types of the pipettes are given in the Sutter manual.

3. **Microforge**: It is also recommended to fire-polish the tip of the pipette to generate a smooth glass surface that makes a good seal to the plasma membrane. This is done by bringing the tip of the pipette to the vicinity of a heated glass ball for a very a fraction of a second using a microforge. Similar technique is routinely used for preparing microelectrodes for electrophysiological recordings.
4. **Filling the Micropipette**: Micropipettes should be filled with a physiological saline solution, such as PBS or non-fluorescent growth media. Importantly the solution should be supplemented with 30% serum that will allow the cell membrane to move smoothly into the pipette. Two approaches can be used to get rid of air bubbles in the tip of the pipette: (i) a tip of the pipette can be immersed in the solution first to allow the liquid to fill the tip by the capillary forces followed by backfilling the pipette from the other end or (ii) the whole pipette can be filled from the back end by gently tapping on the shank of the pipette to remove the bubbles from the tip.
5. **Note**: Pipettes have to be prepared on the day of the experiment.

2. Preparation of Cells

1. **Seeding the cells**: Microaspiration is performed on single cells that are either maintained in suspension or are attached to the substrate. To aspirate cells in suspension, cells are lifted from their substrates and pipetted into a shallow longitudinal chamber that is mounted on the inverted microscope right before the experiment. To aspirate substrate-attached cells, cells are seeded on small cover-slips (~10 mm diameter) that can also be placed into the microaspiration chamber before the experiment. The rationale to use a shallow longitudinal chamber is to allow a micropipette to approach the cells at a very shallow angle, as close to horizontal as possible. This is done to allow the membrane pulled into the micropipette to be visualized on a single plane of focus (see **Figure 2**).
2. **Visualizing cell membrane**: To observe the membrane projection into the pipette, cellular membranes are stained with a lipophilic fluorescent dye, such as dil using a standard staining protocol.
    1. Warm PBS solution.
    2. Dilute the stock dil to a working concentration (5 μM) with the warmed PBS solution.
    3. Sonicate for 5 min to break dye aggregates.
    4. Spin down for 5 min and take supernatant.
    5. Wash cells in PBS 3 times, 5 min each.
    6. Incubate cells with the dye solution for 30 min in a 37 °C incubator.
    7. Wash the cells with PBS 3 times for 5 min each.

3. **Note:** It is possible to substitute dil staining of the membrane with visualizing the sub-membrane cytoskeleton that is also being pulled together with the membrane into the pipette. It needs to be taken into the account, however, that perturbing the cytoskeleton may alter the biomechanical properties of the cell. Moreover, when performing microaspiration experiments with substrate attached cells, it is recommended to use 3D imaging to estimate the length of membrane projection into the pipette that is positioned at an angle to the focal plane of the cells.

3. Microaspiration and Image Acquisition

Equipment: Inverted Fluorescent Microscope, preferably with 3D deconvolution capabilities (Zeiss Axiovert 200M with computer controlled Z-axis movement of the objectives or an equivalent); videocamera connected to a computer (AxioCam MRm or an equivalent), Pressure Transducer (BioTek or an equivalent), Vibration-free station (TMD or an equivalent), Micromanipulator (Narishige, Sutter, Burleigh or equivalent; manipulators can be mechanical, hydraulic or piezoelectric). It is also important to emphasize that microaspiration can be performed using a microscope without 3D capabilities to estimate the stiffness of cells in suspension, such as red blood cells [1,2] or neutrophils [3], isolated organelles, such as nuclei [4] or artificial liposomes [5].

Image Acquisition software: Zeiss AxioVision or an equivalent.

1. **Mount the cells** into a microaspiration chamber, as described above, on an inverted fluorescent microscope. Position the cells choosing a cell for an experiment and place it in the center of the visual field. It is important to perform these experiments in a vibration-free environment, particularly for the experiments with substrate-attached cells because minute vibrations that typically occur on benches and regular tables are likely to completely compromise the creation of the seal, break the tip of the micropipette or result in significant shifts in the position of the tip that will skew the analysis of the results.
2. **Place a micropipette** filled with PBS/media w/ serum solution into a pipette holder connected to a power transducer by flexible tubing with the diameter adjusted to the connecter of the pipette holder for a tight fit. In the beginning of each experiment the pressure in the pipette is equilibrated to the atmospheric pressure. The pipette is mounted onto a micromanipulator that allows fine control of the pipette movements in a micron range. Position a pipette at a shallow angle to the bottom of the chamber and bring the tip of the pipette to the center of the visual field. The shank of the pipette, a cylindrical part of the pipette tip into which the membrane is aspirated, is aligned horizontally to the focal plane by (1) positioning the pipette at the shallowest angle possible (10-15°) and (2) by flexing the shank of the pipette against the bottom of the chamber. Because the shank is very thin it is flexible enough to slide on the bottom of the chamber while approaching a cell, as shown schematically in **Figure 1**. Slowly bring down the micropipette to the side of a single cell using the course manipulator until near the plane of focus for the cell. Then, using a fine manipulator move the micropipette to the edge of the cell until the tip of the pipette gently touches the membrane. Take one image to observe the position of the pipette. Good seals are created when the whole tip of the pipette is in full contact with the cell surface and the contact is stable. There is no strong objective criterion, however, about how good the seal is except for the visual examination.
3. **Apply a step of negative pressure** using the transducer and maintain it until membrane projection is stabilized. The amount of pressure needed to aspirate the membrane into the pipette varies depending on cell type and specific experimental conditions. In our experiments,

initial deformation is typically observed when applying pressure in the range between -2 to -15mm Hg. When the pressure is applied, the membrane is gradually deformed into the pipette until it is stabilized at certain length, a process that typically takes 2-3 min. During this time, images of membrane deformation are acquired every 30 sec to track the progression of the membrane that is pulled into the pipette.

4. **Increase the pressure** to the next level in 2-5 mm Hg steps and repeat the whole procedure until membrane projection detaches from the cell and moves into the pipette, at which point the experiment is stopped.

4. Analysis

To quantify the degree of membrane deformation, the aspirated length (L) is measured from the tip of the pipette to the vertex of the circumference of the membrane projection. It is important to note, however, that a larger pipette will apply more force on the cell membrane at the same level of pressure. To account for the variability between the diameters of the pipettes, therefore, the aspirated length is normalized for the pipette diameter (D) measured for each experiment.

The data can be further analyzed using a standard linear viscoelastic half-space model of the endothelial cell, as described in the earlier studies [6,7]. Specifically, the elastic modulus of the cells was estimated using the equation:

$$E = \frac{3a\Delta p}{2\pi L}\phi(\eta)$$

where E is Young's modulus, a is the inner radius of the pipette, Δp is the pressure difference, L is the corresponding aspirated length, and $\varphi(\eta)$ is a wall function calculated using the force model, as described by Theret *et al* [7]. It is important to note that multiple models have been used to analyze the microaspiration data including a finite element model that assumes that a cell is a deformable sphere with isotropic and homogenous material properties and liquid drop models, which assume that cells form a spherical shape, can deform continuously, and recover upon release, as described in several excellent reviews: [8-10]. Microaspiration can also be used to investigate other biomechanical parameters of cells and tissues, such as cellular viscoelastic properties, cortical tension and contribution of different structural elements to cell and tissue biomechanics (see the reviews listed above for more information).

5. Representative Results

In earlier studies, micropipette aspiration was performed either on liposomes [5] or on cells that were not attached to the substrate [2,11-13]. In our studies, however, the cells are typically maintained attached to the substrate to avoid changes in the cytoskeletal structure that are likely to occur when cells detach [14-16]. To validate the use of microaspiration technique for substrate-attached cells, we tested whether disruption of F-actin results in the decrease in cell stiffness of bovine aortic endothelial cells (BAECs), as estimated by this approach. **Figure 3** shows that, as expected, this is indeed the case. Specifically, **Figure 3A** shows a typical series of fluorescent images of an endothelial membrane undergoing progressive deformation in response to negative pressure applied through a micropipette. As expected, the membrane is gradually aspirated into the pipette and the aspirated length increases as a function of applied pressure. The time-courses of the deformation show that disruption of F-actin significantly increases the aspirated lengths of the projections under all pressure conditions (**Figure 3B**) [14].

Using this approach, we discovered that cell stiffness increases when cellular membranes are depleted of cholesterol whereas cholesterol enrichment had no effect [14]. **Figure 4** shows a cholesterol-enriched cell, a control cell, and a cholesterol-depleted cell after reaching maximal aspiration lengths at -15 mm Hg (4A). The projections typically started to develop at -10mmHg and the time-courses of membrane deformation could be measured for the negative pressures of -10, -15 and -20 mm Hg (4B). Application of pressures above -25mmHg resulted in detachment of the aspirated projection forming a separate vesicle. The pressure level that resulted in membrane detachment was similar under different cholesterol conditions. This observation was highly unexpected because previous studies showed that in membrane lipid bilayers an increase in membrane cholesterol increases the stiffness of the membrane [5,17]. Our further studies confirmed these observations using several independent approaches, including Atomic Force Microscopy [18,19] and Force Traction Microscopy [20].

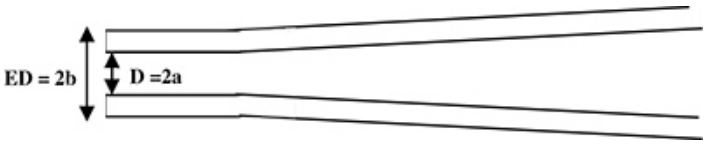

Figure 1. Schematic side view of a recording pipette. The pipette is pulled to generate a cylindrical shank at the tip (side view). Micropipette parameters: D=2a=internal diameter and ED=2b=external diameter.

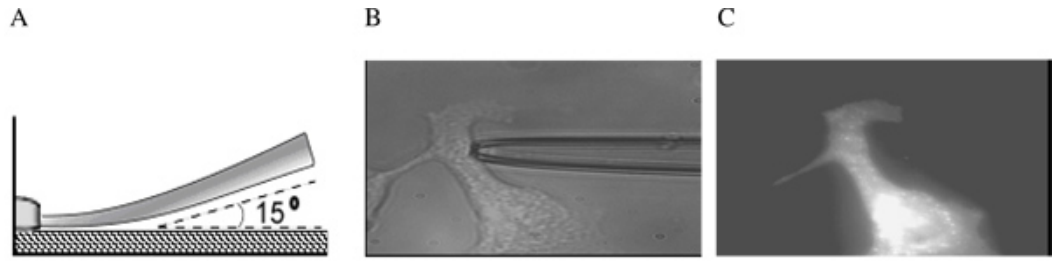

Figure 2. Micropipette approaching a substrate-attached cell. (A) Schematic side view; (B) Bright contrast image of a micropipette shank touching a typically shaped cell used in aspiration experiments; (C) Fluorescent image of the same cell labeled with $DiIC_{18}$. The micropipette is still present but is invisible (From [14]).

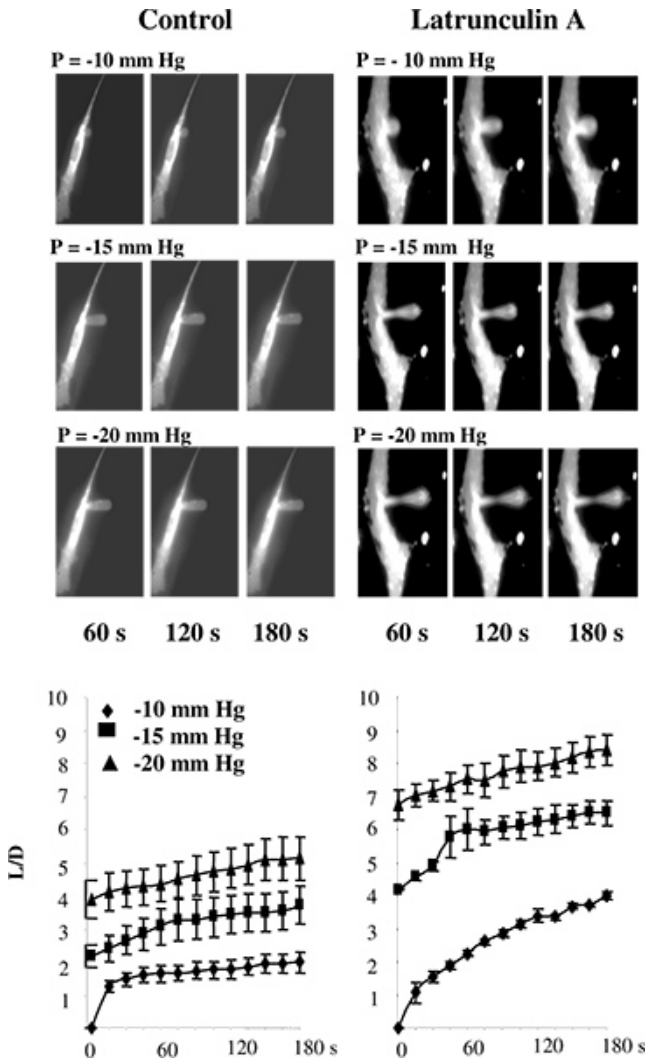

Figure 3. Validation of measuring cell stiffness in substrate-attached cells using microaspiration. A: Images of progressive membrane deformation of BAECs under control conditions and after exposure to latrunculin. The pipette is invisible on the images because it does not fluoresce. The cells were exposed to 2 μM latrunculin A for 10 min, which dramatically reduced the amount of F-actin, as measured by rhodamine-phalloidin fluorescence (not shown) but had no significant effect on the cell shape. In a latrunculin-treated cell, there is a thinning of the membrane in the middle of the aspirated projection but the projection is still attached to the cells. **B**. Effect of latrunculin A on the time courses of membrane deformation where L is aspirated length of the membrane projection and D is the diameter of the pipette for control cells (n=14) and cells exposed to 2 μM latrunculin A for 10 min (n=5). The cells were aspirated with -10 mm Hg (diamonds), -15 mm Hg (squares) and -20 mm Hg (triangles). (From [14].)

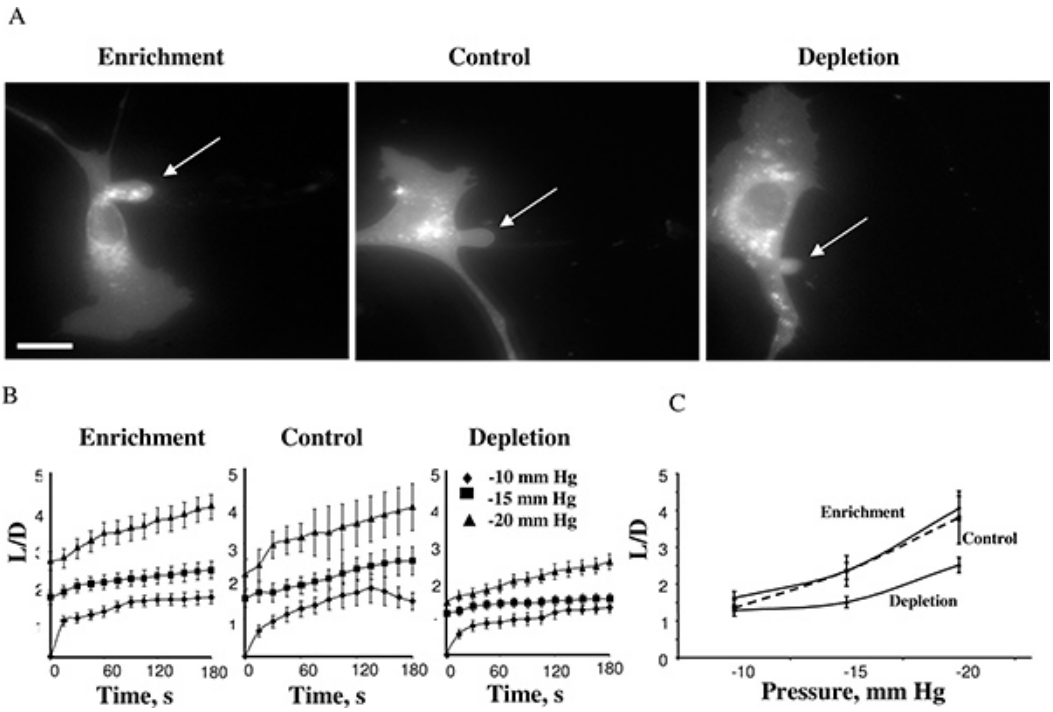

Figure 4. Effect of cellular cholesterol levels on membrane deformation of BAECs. A. Typical images of membrane deformation of cholesterol-enriched, cholesterol-depleted and control cells (control cells were exposed to MβCD:MβCD-cholesterol mixture at 1:1 ratio that had no effect on the level of free cholesterol in the cells (see inset). The images shown depict the maximal deformation at -15 mm Hg. The arrow indicates the position of the aspirated projection. The bar is 30 μm. **B**. Average time-courses of aspirated lengths for the three experimental cell populations. **C**. Maximal aspirated lengths plotted as a function of the applied pressure. The maximal normalized length in depleted cells was significantly lower than that of control cells for pressures -15 mm Hg and -20 mm Hg ($P < 0.05$). (From [14].)

Discussion

Microaspiration provides a simple and highly reproducible method to estimate cell stiffness/deformability by applying negative pressure to a cell membrane and measuring membrane deformability in response to well-defined pressure. It was first developed by Mitchison and Swann (1954) to characterize the elastic properties of sea-urchin eggs to provide insights into the mechanisms of cell division [21] and then to look at the mechanical properties in red blood cells [1]. This method has been used in multiple studies to assess the biomechanical properties of various cell types (*e.g.* [2,3,12,13]). Our recent studies extended this method to estimate the stiffness of substrate-attached cells by combining microaspiration with 3D imaging [14,15,22]. Membrane stiffness and elasticity provide critical information regarding cell phenotype and how cells respond to a dynamic environment, particularly to a variety of mechanical clues that are generated by hemodynamic forces of the blood flow or by changing the viscoelastic properties of the extracellular matrix. Indeed, earlier studies have shown that cell stiffness increases in response to fluid shear stress [13,23] and as a function of the stiffness of the substrate [16,24]. Changes in cell stiffness are expected to have a major impact on cell mechanosensitivity and mechanotransduction. Specifically, we have shown recently that an increase in endothelial stiffness facilitates their sensitivity to flow [25]. We have also shown that endothelial stiffening is associated with an increase in their angiogenic potential [22]. Furthermore, a decrease in membrane stiffness and viscosity characterize proliferative late-stage ovarian cancer cells indicating that these properties can help differentiate early stage versus an aggressive malignant phenotype [26].

Measuring cell stiffness also may provide major insights into the structure and organization of the cytoskeleton. A key factor in determining cell stiffness is the sub-membrane cytoskeleton, particularly F-actin [6,14]. Changes in cell stiffness may also reflect cytoskeletal re-arrangement in response to different signaling events, such as activation of Rho-GTPases [27], a major mechanism that couple between the membrane and the cytoskeleton [28]. Furthermore, changes in cell stiffness can be detected even when no obvious changes in the structure of the cytoskeleton networks are observed [14] suggesting that this approach is more sensitive to subtle changes in the cytoskeleton structure than visualization of the networks.

In terms of alternative approaches, microaspiration provides a useful and inexpensive alternative to Atomic Force Microscopy (AFM) that is typically used to measure cell stiffness [29,30]. In contrast to AFM that measures local membrane rigidity, microaspiration provides a global measure of the deformability of a cell. Other methods to estimate cellular biomechanical properties include various bead/particle approaches, such as magnetic twisting cytometry [31-33], particle tracking [34,35], as well as several other approaches, such as cytoindenter, a method that is somewhat similar to the AFM [36] and optical tweezers [37]. While detailed comparative analysis of these techniques is beyond the scope of this manuscript, the main differences between them and microaspiration are the following: (i) Magnetic twisting cytometry involves applying an external force to a bead attached to the cells surface to cause local membrane deformation at the site where the bead is attached which is most important to determine the force-induced stiffening response [31]; (ii) Particle tracking can be used for several different purposes, such as estimating the force that cells exert on the substrate (Traction Force Microscopy) [34] or estimate the stiffness of the internal "deep" layers of the cell by analyzing the motion of the beads or organelles inside the cell [35]. In contrast, optical tweezesrs are used to pull membrane nanotubes (tethers) to estimate cortical tension and membrane-cytoskeleton adhesion [37]. An alternative method to pull membrane tethers is to use the AFM, a method that has both significant similarities and differences as compared to optical tweezers [18,38]. The advantage of most of these methods

is that they may provide detailed spatial information about the biomechanical properties of the individual cells. However, all of these techniques require either very expensive equipment or sophisticated and not readily available software packages. The strength of the microaspiration, on the other hand, is that it is a good as other methods at providing quantitative results and differentiating among specific mechanical models of the cell without the requirement of the highly specialized equipment or software. In summary, while there are multiple approaches to assess the biomechanical properties of cells and tissues, microaspiration remains a useful and powerful approach to investigate cellular biomechanics.

Disclosures

No conflicts of interest declared.

References

1. Rand, R.P. & Burton, A.C. Mechanical properties of the red cell membrane. I. Membrane stiffness and intracellular pressure. *Biophys. J.* **4**, 115-135 (1964).
2. Discher, D.E., Mohandas, N., & Evans, E.A. Molecular maps of red cell deformation: hidden elasticity and in situ connectivity. *Science.* **266**, 1032-1035 (1994).
3. Schmid-Schönbein, G.W., Sung, K.L., Tözeren, H., Skalak, R., & Chien, S. Passive mechanical properties of human leukocytes. *Biophys. J.* **36**, 243-256 (1981).
4. Guilak, F., Tedrow, J.R., & Burgkart, R. Viscoelastic properties of the cell nucleus. *Biochem. Biophys. Re.s Commun.* **269** (3), 781-786 (2000).
5. Needham, D. & Nunn, R.S. Elastic deformation and failure of lipid bilayer membranes containing cholesterol. *Biophys. J.* **58** (4), 997-1009 (1990).
6. Sato, M., Theret, D.P., Wheeler, L.T., Ohshima, N., & Nerem, R.M. Application of the micropipette technique to the measurement of cultured porcine aortic endothelial cell viscoelastic properties. *Journal of Biomechanical Engineering*. **112** (3), 263-268 (1990).
7. Theret, D.P., Levesque, M.J., Sato, F., Nerem, R.M., & Wheeler, L.T. The application of a homogeneous half-space model in the analysis of endothelial cell micropipette measurements. *J. of Biomechanical Engineering*. **110** (3), 190-199 (1988).
8. Hochmuth, R.M. Micropipette aspiration of living cells. *J. Biomech.* **33** (1), 15-22 (2000).
9. Lim, C.T., Zhou, E.H., & Quek, S.T. Mechanical models for living cells--a review. *Journal of Biomechanics*. **39** (2), 195 (2006).
10. Zhao, R., Wyss, K., & Simmons, C.A. Comparison of analytical and inverse finite element approaches to estimate cell viscoelastic properties by micropipette aspiration. *Journal of Biomechanics*. **42** (16), 2768 (2009).
11. Chien, S., Sung, K. L., Skalak, R., Usami, S., & Tozeren, A. Theoretical and experimental studies on viscoelastic properties of erythrocyte membrane. *Biophys. J.* **24** (2), 463-487 (1978).
12. Evans, E. & Kuhan, B. Passive material behavior of granulocytes based on large deformation and recovery after deformation tests. *Blood*. **64** (5), 1028-1035 (1984).
13. Sato, M., Levesque, M.J., & Nerem, R.M. Micropipette aspiration of cultured bovine aortic endothelial cells exposed to shear stress. *Arteriosclerosis*. **7** (3), 276-286 (1987).
14. Byfield, F., Aranda-Aspinoza, H., Romanenko, V.G., Rothblat, G.H., & Levitan, I. Cholesterol depletion increases membrane stiffness of aortic endothelial cells. *Biophys. J.* **87** (5), 3336-3343 (2004).
15. Byfield, F.J., Hoffman, B.D., Romanenko, V.G., Fang, Y., Crocker, J.C., & Levitan, I. Evidence for the role of cell stiffness in modulation of volume-regulated anion channels. *Acta. Physiologica*. **187** (1-2), 285-294 (2006).
16. Byfield, F.J., Reen, R.K., Shentu, T.-P., Levitan, I., & Gooch, K.J. Endothelial actin and cell stiffness is modulated by substrate stiffness in 2D and 3D. *Journal of Biomechanics*. **42** (8), 1114 (2009).
17. Evans, E. & Needham, D. Physical properties of surfactant bilayer membranes: thermal transitions, elasticity, rigidity, cohesion and colloidal interactions. *Journal of Physical Chemistry*. **91** (16), 4219-4228 (1987).
18. Sun, M., Northup, N., Marga, F., Huber, T., Byfield, F.J., Levitan, I., & Forgacs, G. The effect of cellular cholesterol on membrane-cytoskeleton adhesion. *J. Cell. Sci.* **120** (Pt. 13), 2223-2231 (2007).
19. Shentu, T.P., Titushkin, I., Singh, D.K., Gooch, K.J., Subbaiah, P.V., Cho, M., & Levitan, I. oxLDL-induced decrease in lipid order of membrane domains is inversely correlated with endothelial stiffness and network formation. *Am. J. Physiol. Cell. Physiol.* **299** (2), C218-229 (2010).
20. Norman, L.L., Oetama, R.J., Dembo, M., Byfield, F., Hammer, D.A., Levitan, I., & Aranda-Espinoza, H. Modification of Cellular Cholesterol Content Affects Traction Force, Adhesion and Cell Spreading. *Cell Mol. Bioeng.* **3** (2), 151-162 (2010).
21. Mitchinson, J.M. & Swann, M. M. The Mechanical Properties of the Cell Surface: I. The Cell Elastimeter. *J. of Experimental Biology.* **31**, 443-460 (1954).
22. Byfield, F. J., Tikku, S., Rothblat, G.H., Gooch, K.J., & Levitan, I. OxLDL increases endothelial stiffness, force generation, and network formation. *J. Lipid Res.* **47** (4), 715-723 (2006).
23. Ohashi, T., Ishii, Y., Ishikawa, Y., Matsumoto, T., & Sato, M. Experimental and numerical analyses of local mechanical properties measured by atomic force microscopy for sheared endothelial cells. *Biomed. Mater. Eng.* **12** (3), 319-327 (2002).
24. Solon, J., Levental, I., Sengupta, K., Georges, P.C., & Janmey, P.A. Fibroblast adaptation and stiffness matching to soft elastic substrates. *Biophysical Journal*. **93** (12), 4453 (2007).
25. Kowalsky, G.B., Byfield, F.J., & Levitan, I. oxLDL facilitates flow-induced realignment of aortic endothelial cells. Am. J. Physiol. Cell. Physiol. **295** (2), C332-340 (2008).
26. Ketene, A.N., Schmelz, E.M., Roberts, P.C., & Agah, M. The effects of cancer progression on the viscoelasticity of ovarian cell cytoskeleton structures. *Nanomedicine: Nanotechnology, Biology and Medicine*., In Press, Corrected Proof, (2011).
27. Kole, T.P., Tseng, Y., Huang, L., Katz, J.L., & Wirtz, D. Rho kinase regulates the intracellular micromechanical response of adherent cells to rho activation. *Mol. Biol. Cell.* **15** (7), 3475-3484 (2004).
28. Hall, A. Rho GTPases and the Actin Cytoskeleton. *Science.* **279** (5350), 509-514 (1998).
29. Okajima, T. Atomic Force Microscopy for the Examination of Single Cell Rheology. In Press., *Curr. Pharm. Biotechnol.*, (2011)
30. Azeloglu, E.U. & Costa, K.D. Atomic force microscopy in mechanobiology: measuring microelastic heterogeneity of living cells. *Methods Mol. Biol.* **736**, 303-329 (2011).

31. Wang, N., Butler, J.P., & Ingber, D.E. Mechanotransduction across the cell surface and through the cytoskeleton. *Science*. **260** (5111), 1124-1127 (1993).
32. Fabry, B., Maksym, G.N., Butler, J.P., Glogauer, M., Navajas, D., & Fredberg, J.J. Scaling the microrheology of living cells. *Physical Review Letters.* **87** (14), 148102 (2001).
33. Park, C.Y., Tambe, D., Alencar, A.M., Trepat, X., Zhou, E.H., Millet, E., Butler, J.P., & Fredberg, J.J. Mapping the cytoskeletal prestress. *American Journal of Physiology - Cell Physiology*. **298** (5), C1245-C1252 (2010).
34. Munevar, S., Wang, Y., & Dembo, M. Traction force microscopy of migrating normal and H-ras transformed 3T3 fibroblasts. *Biophys. J.* **80** (4), 1744-1757 (2001).
35. Wirtz, D. Particle-tracking microrheology of living cells: principles and applications. *Annu. Rev. Biophys.* **38**, 301-326 (2009).
36. Shin, D. & Athanasiou, K. Cytoindentation for obtaining cell biomechanical properties. *J. Orthop. Res.* **17** (6), 880-890 (1999).
37. Ou-Yang, H.D. & Wei, M.T. Complex fluids: probing mechanical properties of biological systems with optical tweezers. *Annu. Rev. Phys. Chem.* **61**, 421-440 (2010).
38. Hosu, B.G., Sun, M., Marga, F., Grandbois, M., & Forgacs, G. Eukaryotic membrane tethers revisited using magnetic tweezers. Phys. Biol. **4** (2), 67-78 (2007).

